Journal of Organometallic Chemistry 894 (2019) 18–27

Contents lists available at ScienceDirect

Journal of Organometallic Chemistry

journal homepage: www.elsevier.com/locate/jorganchem

Green, effective and chromatography free synthesis of benzoimidazo [1,2-*a*]pyrimidine and tetrahydrobenzo [4,5]imidazo [1,2-*d*] quinazolin-1(2*H*)-one and their pyrazolyl moiety using Fe_3O_4@SiO_2@*L*-proline reusable catalyst in aqueous media

Leila Zare Fekri [a, *], Mohammad Nikpassand [b], Samira Nazari Khakshoor [c]

[a] Department of Chemistry, Payame Noor University, PO Box,19395-3697, Tehran, Iran
[b] Department of Chemistry, Rasht Branch, Islamic Azad University, Rasht, Iran
[c] Ghadr Institute of Higher Education, Department of Pharmaceutical Chemistry, Koochesfahan, Guilan, Iran

ARTICLE INFO

Article history:
Received 31 March 2019
Received in revised form
26 April 2019
Accepted 3 May 2019
Available online 6 May 2019

Keywords:
Benzoimidazo[1,2-*a*]pyrimidine
Tetrahydrobenzo [4,5]imidazo-[1,2-*d*] quinazolin-1(2*H*)-one
Fe_3O_4@SiO_2@*L*-proline
Reusable catalyst
Aqueous media

ABSTRACT

L-proline-functionalized silica-coated Fe_3O_4 nanoparticle was synthesized and characterized using Fourier Transform infrared spectroscopy (FT-IR), X-ray diffraction (XRD), field emission scanning electron microscopy (FE-SEM), transmission electron microscopy (TEM), energy dispersive X-ray spectroscopy (EDS), thermogravimetric analysis (TGA), Zeta potential and a vibrating sample magnetometer (VSM). The Fe_3O_4@SiO_2@*L*-proline nanoparticles in aqeous media have been used as a green avenue for the mild and efficient multicomponent synthesis of new derivatives of benzoimidazo[1,2-*a*]pyrimidines and tetrahydrobenzo [4,5]imidazo-[1,2-*d*]quinazolin-1(2*H*)-ones in excellent yields. Furthermore, the recovery and reuse of the catalyst was demonstrated 10 times without a detectible loss in activity. Eco-friendliness, high purity of the desired products, short reaction time and easy workup can be mentioned as the other advantages of this method.

1. Introduction

Benzoimidazo[1,2-*a*]pyrimidines are important biologically active heterocyclic compounds, which possess pharmaceutical properties such as antineoplastic [1], anticancer [2], antifungal [3], anti-inflammatory [4], antiviral [5], antimicrobial [6], antitubercular [7], calcium channel blockers [8], parasitical activity [9], benzodiazepine receptor agonists [10], potent P38 MAP kinase inhibitors [11], protein kinase inhibitor [12], TIE-2 and/or VEGFR2 inhibitory activities [13] and T cell activation [14].

There were several approaches to develop the benzimidazo[1,2-*a*]pyrimidinones: the intramolecular substitution reaction of halide with amines [15], the reaction of 2-amino benzimidazole with propionic esters and α,β-unsaturated esters [16], the one-pot three-component condensation reactions of β-dicarbonyl compounds, aldehyde and 2-amino benzimidazole in the presence of catalyst [17,18], the reactions of 2-aminobenzimidazole with several electrophiles, including nitrile, α,β-unsaturated carbonyl compounds, cyanoacetate, acetylene-dicarboxylate [19] and the reaction of 2-aminobenzimidazole with Baylis–Hillman adducts and their derivatives [20].

However, most of these procedures have significant drawbacks such as low yields, difficult work-up, long reaction times, harsh reaction conditions and use of environmentally toxic reagents or media. Thus, we need still a simple and general avenue for one-pot synthesis of benzoimidazo[1,2-*a*]pyrimidine derivatives under mild conditions.

Today, catalysts play a significant role in the production of chemicals and nano catalysts have the potential for improving efficiency, selectivity and yield of the catalytic process. The higher surface to volume ratio means that more catalyst actively participates in the reaction. The potential for cost saving in the scope of material, equipment, labour and time are the other benefits of nano catalysts. Higher selectivity means less waste and fewer impurities, which could lead to safer and reduced environmental impact [21]. On the other hands, traditional heterogeneous catalysts are limited

* Corresponding author.
E-mail addresses: chem_zare@yahoo.com, chem_zare@pnu.ac.ir (L.Z. Fekri).

https://doi.org/10.1016/j.jorganchem.2019.05.004
0022-328X/

in the nature of their active sites and their reaction scope abilities. Soluble organic catalysts can catalyse a variety of reaction more than traditional solid catalysts but suffer from their inability (or high degree of difficulty) to be recycled. For this reason, synthesis of organic and inorganic hybrid composite to utilize the organic moiety as the active site and the solid to provide avenue to recovery and recyclability is attractive. These hybrids can be synthesized by a number of methods: (i) adsorption of the organic species into the pores of the support; (ii) construction of the organic molecule piece by piece within the confines of cavities of the support (the "ship-in-bottle" technique); (iii) attachment of the desired functionality to the support by covalent bond formation; (iv) direct synthesis into the final composite material. Here, we specifically address the use of organic-inorganic hybrid materials based on nano Fe_3O_4 nanoparticles for use as catalysts [22].

2. Experimental

2.1. Materials and instruments

Chemicals were purchased from Merck and Fluka. All solvents used were dried and distilled according to standard procedures. Melting points were measured on an Electrothermal 9100 apparatus. IR spectra were determined on a Shimadzu FT-IR 8600 spectrophotometer. ^1H and ^{13}C NMR spectra were determined on a Bruker 300 DRX Avance instrument at 300 and 75 MHz. Elemental analyses were recorded on a Carlo-Erba EA1110CNNO-S analyser. Nanostructures were detected using a Philips Xpert X-ray powder diffraction (XRD) diffractometer (CuKα, radiation, $\lambda = 0.154056$), at a scanning speed of 2°/min from 10° to 80° (2θ). Transmission electron microscopy (TEM) measurements were carried out on a Zeiss-EM10C-100 KV instrument. Thin layer chromatography (TLC) was carried out with ethyl acetate: n-hexane 1:4 on TLC Silica gel 60 F_{254}.

2.2. Synthesis of Fe_3O_4 nanoparticles

First, $FeCl_3 \cdot 6H_2O$ and $FeCl_2 \cdot 4H_2O$ with molar proportion of 1:2 were dissolved in ethanol or deionized water and then NaOH solution (3 mol L^{-1}) was added into the above solution using a peristaltic pump under constant magnetic stirring for 30 min, and the final pH was 10. Afterwards, the sodium citrate and oleic acid were respectively added into the suspensions to modify the obtained Fe_3O_4 MNPs for 12 h. The substance obtained were digested at maintained temperature for 30 min and cooled at room temperature. The resulting particles were magnetically separated and washed repeatedly with deionized water and ethanol until pH was 7. The products were then dried at 60 °C in vacuum for 6 h for further characterizations.

2.3. Synthesis of Fe_3O_4@SiO_2@Cl MNPs

500 mg Fe_3O_4 nanoparticles were dispersed into 50 mL toluene and sonicated for 20 min, followed by the addition of 0.5 mL (3-chloropropyl)trimethoxysilane (CPTES). Then, the mixture was refluxed at 110 °C with continuous stirring for 12 h under a nitrogen flow. The resulting Fe_3O_4@SiO_2-Cl MNPs was collected by magnetic separation followed by washing with toluene and ethanol several times and drying at 60 °C for 6 h.

2.4. Synthesis of Fe_3O_4@SiO_2@L-proline

500 mg Fe_3O_4@SiO_2@Cl MNPs were dispersed into 50 ml toluene and sonicated for 30 min, followed by the addition of 0.5 g L-proline. Then, the mixture was refluxed at 110 °C with continuous stirring for 12 h under a nitrogen flow. The resulting functionalized Fe_3O_4@SiO_2@L-proline was collected by magnetic separation followed by washing with toluene and ethanol several times and drying at 80 °C for 8 h.

2.5. General procedure for preparation of benzoimidazo[1,2-a] pyrimidine and tetrahydrobenzo[4,5]imidazo [1,2-d]quinazolin-1(2H)-one

A mixture of aldehyde **1** (1.0 mmol), 2-aminobenazimidazole **2** (1 mmol), indanedione **3** or dimedone **4** (1.0 mmol) and 0.05 g Fe_3O_4@SiO_2@L-proline in 10 mL water was stirred for the required reaction time according to Table 2. After completion of the reaction, as indicated by TLC (TLC Silica gel 60 F_{254}, ethyl acetate: *n*-hexane 1: 4), the resulting mixture was filtered in the presence of an enormous magnetic bar to separate the catalyst from product. The catalyst was washed with hot distilled water (5 mL) and ethanol (3 mL) two times and reused in the next run. The product needs no more recrystallization or column chromatography for purification.

2.5.1. 12-(4-nitrophenyl)-5H-benzo[4,5]imidazo[1,2-a]indeno[1,2-d]pyrimidin-13(12H)-one (5a)

m.p.: 202–204 °C; FT-IR (KBr) (ν_{max}/cm^{-1}): 3431 (N-H stretching), 3060 (aromatic C-H stretching), 2918 (aliphatic C-H stretching), 1745 (C=O stretching), 1608 (aromatic C=C stretching), 1570 (asymmetric NO_2 stretching), 1494 (aromatic C=C stretching), 1388 (symmetric NO_2 stretching), 1245 (C-N stretching) cm^{-1}; ^{1}H NMR (DMSO-d_6, 300 MHz): δ_H (ppm) 5.39 (s, 1H), 7.15–7.21 (m, 2H), 7.25 (d, $J = 7.5$ Hz, 2H), 7.39 (d, $J = 8.7$ Hz, 3H), 7.49 (s, 2H), 7.57 (t, $J = 5.4$ Hz, 2H), 7.63 (m, 1H) ppm. ^{13}C NMR (DMSO-d_6, 75 MHz): δ_C (ppm) 62.66, 111.12, 117.46, 119.23, 121.76, 125.09, 129.54, 130.02, 130.48, 131.45, 131.98, 133.09, 133.89, 134.95, 135.21, 139.07, 139.47, 140.14, 145.54, 158.67, 192.54 ppm. Anal Calc. for $C_{23}H_{14}N_4O_3$: C, 70.05; H, 3.58; N, 14.21. Found: C, 70.01; H, 3.55, N, 14.22.

Table 1
Optimization of reaction condition.

entry	Reaction solvent	temperature	Catalyst amount (g)	Time (min)	Yield (%)
1	Solvent-free	rt	0.05	10	94
2	DMF	rt	0.05	90	72
3	EtOH	rt	0.05	60	83
4	CH_3CN	rt	0.05	300	56
5	H2O–EtOH (1:1)	rt	0.05	45	81
6	toluene	rt	0.05	600	trace
7	H_2O	rt	0.05	10	97
8	H_2O	60 °C	0.05	10	97
9	H_2O	rt	0.01	60	82
10	H_2O	rt	0.1	10	94

Table 2
Synthesis of benzimidazo [1,2-a]pyrimidinone and tetrahydrobenzo[4,5]imidazo-[1,2-d]quinazolin-1(2H)-one using Fe_3O_4@SiO_2@L-proline MNPs.

Product	Structure	Time (min)	Yield (%)[a,b]	Mp (°C)	Product	Structure	Time (min)	Yield (%)[a,b]	Mp (°C)
5a	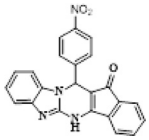	10	97	202–204	6a	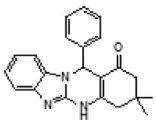	12	96	234–236
5b	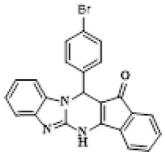	12	96	234–236	6b	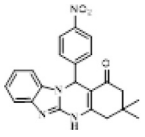	10	96	257–259
5c	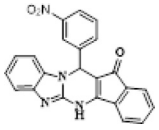	12	96	237–239	6c	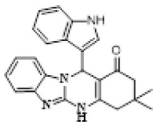	12	92	221–223
5d	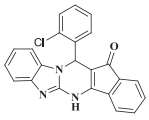	15	90	276–277	6d	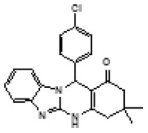	10	95	199–201
5e	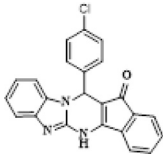	12	95	256–258	6e	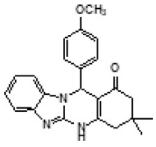	15	94	234–235
5f	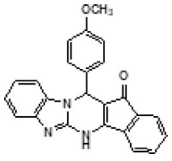	17	90	189–190	6f	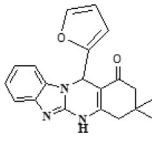	10	95	214–216

[a] Isolated yield.
[b] All of synthesized compounds are known and were characterized by mp, FT-IR, NMR and elemental analysis.

2.5.2. 12-(4-bromophenyl)-5H-benzo[4,5]imidazo[1,2-a]indeno [1,2-d]pyrimidine-13-(12H)-one (5b)

m.p.: 234–236 °C; FT-IR (KBr) (ν_{max}/cm^{-1}): 3465 (N-H stretching), 3037 (Aromatic C-H stretching), 1737 (C=O stretching), 1608 (aromatic C=C stretching), 1552, 1483 (aromatic C=C stretching), 1386 (C-N) 1068 (C-Br Stretching) cm^{-1}; ^{1}H NMR (DMSO-d_6, 300 MHz): δ_H (ppm) 4.47 (s, 1H, C-H), 6.83–6.87 (m, 3H), 7.08–7.09 (m, 3H), 7.10 (dd, J = 3.6 Hz, J = 5.4 Hz, 3H), 7.29 (d, J = 8.4 Hz, 2H), 7.52 (dd, J = 2.1 Hz, J = 6.6 Hz, 1H), 11.29 (brs, NH, 1H) ppm. ^{13}C NMR (DMSO-d_6, 75 MHz): δ_C (ppm) 62.59, 111.98, 119.39, 119.99, 120.43, 126.58, 129.06, 129.82, 130.36, 130.62, 130.86, 131.108, 131.71, 131.95, 132.19, 132.67, 139.47, 139.64, 141.75, 159.24, 191.46 ppm. Anal Calc. for $C_{23}H_{14}BrN_3O$: C, 64.50; H, 3.29; N, 9.81. Found: C, 64.51; H, 3.23, N, 9.84.

2.5.3. 12-(3-nitrophenyl)-5H-benzo[4,5]imidazo[1,2-a]indeno[1,2-d]pyrimidine-13-(12H)-one (5c)

m.p.: 237–239 °C; FT-IR (KBr) (ν_{max}/cm^{-1}): 3400 (N-H stretching), 3091 (aromatic C-H stretching) 1726 (C=O stretching), 1606 (aromatic C=C stretching), 1529 (asymmetric NO_2 stretching), 1348 (C-N stretching) cm^{-1}; ^{1}H NMR (DMSO-d_6, 300 MHz): δ_H (ppm) 5.23 (s, 1H), 7.21 (dd, J = 3.3 Hz, J = 6.0 Hz, 1H), 7.37 (dd, J = 3.2 Hz, J = 5.7 Hz, 1H), 7.48–7.55 (m, 2H), 7.67 (brs, 1H), 7.74–7.79 (m, 2H), 7.83 (d, J = 7.8 Hz, 1H), 7.94 (s, 1H), 7.95–8.04 (m, 2H), 8.15 (d, J = 9.3 Hz, 1H), 12.5 (brs, N-H, 1H) ppm. ^{13}C NMR (DMSO-d_6, 75 MHz): δ_C (ppm) 59.14 (C-H), 111.82, 123.48, 123.72, 123.88, 124.21, 127.18, 127.50, 127.67, 130.08, 131.93, 132.25, 133.27, 134.45, 136.66, 136.74, 140.14, 140.25, 142.49, 142.71, 148.25, 156.72, 188.93 (C=O) ppm. Anal Calc. for $C_{23}H_{14}N_4O_3$: C, 70.05; H, 3.58; N, 14.21. Found: C, 70.08; H, 3.53, N, 14.24.

2.5.4. 12-(2-chlorophenyl)-5H-benzo[4,5]imidazo[1,2-a]indeno [1,2-d]pyrimidine-13-(12H)-one (5d)

m.p.: 276–277 °C; FT-IR (KBr) (ν_{max}/cm^{-1}): 3417 (N-H stretching), 1712 (C=O stretching), 1604, 1460 (aromatic C=C stretching), 1375 (C-N stretching), 1078 (C-Cl stretching) cm^{-1}; ^{1}H NMR (DMSO-d_6, 300 MHz): δ_H (ppm) 5.01 (s, 1H), 6.94 (dd, J = 3.0 Hz, J = 5.4 Hz, 2H), 7.10 (d, J = 8.7 Hz, 1H), 7.16–7.19 (m, 3H), 7.25–7.31 (m, 2H), 7.43–7.53 (m, 3H), 7.82–7.88 (m, 1H) ppm. ^{13}C NMR (DMSO-d_6, 75 MHz): δ_C (ppm) 56.71, 111.90 (two peaks), 114.90, 120.49 (two peaks), 124.71, 125.63 (two peaks), 127.41 (two peaks), 132.28, 133.58, 136.76 (two peaks), 139.38, 142.47, 144.43, 144.96, 154.76 (two peaks), 156.93, 191.78 ppm. Anal Calc. for $C_{23}H_{14}ClN_3O$: C, 71.97; H, 3.68; N, 10.95. Found: C, 71.98; H, 3.63, N, 10.92.

2.5.5. 12-(4-chlorophenyl)-5H-benzo[4,5]imidazo[1,2-a]indeno [1,2-d]pyrimidine-13-(12H)-one (5e)

m.p.: 256–258 °C; FT-IR (KBr) (ν_{max}/cm^{-1}): 3392 (N-H stretching), 3089 (aromatic C-H stretching), 2866 (aliphatic C-H stretching), 1728 (C=O stretching) 1606 (aromatic C=C stretching), 1529, 1448 (aromatic C=C stretching), 1307 (C-N Stretching), 1097 (C-Cl stretching) cm^{-1}; ^{1}H NMR (DMSO-d_6, 300 MHz): δ_H (ppm) 5.10 (s, 1H, C-H), 7.39–7.48 (m, 2H), 7.57 (m, 1H), 7.59 (m, 2H), 7.65–7.66 (m, 3H), 7.70–7.79 (m, 2H), 7.80–7.89 (m, 2H) ppm. ^{13}C NMR (DMSO-d_6, 75 MHz): δ_C (ppm) 61.34, 111.56, 114.66, 120.77, 123.18, 127.50, 129.01, 129.17, 130.21, 130.64, 131.56, 131.94, 132.33, 133.09, 133.37, 135.87, 139.45, 145.66, 146.75, 158.88, 186.86 ppm. Anal Calc. for $C_{23}H_{14}ClN_3O$: C, 71.97; H, 3.68; N, 10.95. Found: C, 71.95; H, 3.65, N, 10.90.

2.5.6. 12-(4-methoxyphenyl)-5H-benzo[4,5]imidazo[1,2-a]indeno [1,2-d]pyrimidine-13-(12H)-one (5f)

m.p.: 189–190 °C; FT-IR (KBr) (ν_{max}/cm^{-1}): 3365 (N-H stretching), 3093 (aromatic C-H stretching), 2876 (aliphatic C-H stretching), 1731 (C=O stretching), 1614 (aromatic C=C stretching), 1556, 1446 (aromatic C=C stretching), 1323 (C-N Stretching), 1213 (C-O stretching) cm^{-1}; ^{1}H NMR (DMSO-d_6, 300 MHz): δ_H (ppm) 3.39 (s, 3H), 5.11 (s, 1H, C-H), 7.28 (d, J = 8.3 Hz, 2H), 7.46–7.73 (m, 3H), 7.64 (t, J = 8.3 Hz, 2H), 7.76–7.85 (m, 2H), 7.97 (d, J = 8.3 Hz, 2H), 8.07–8.12 (m, 1H) ppm. ^{13}C NMR (DMSO-d_6, 75 MHz): δ_C (ppm) 54.62, 61.14, 111.98, 114.09, 116.65, 119.18, 123.57, 126.21, 126.83, 128.31, 130.69, 131.43, 133.05, 135.08, 135.79, 136.29, 139.48, 141.05, 144.08, 155.78, 157.23, 186.86 ppm. Anal Calc. for $C_{24}H_{17}N_4O_3$: C, 75.97; H, 4.52; N, 11.08. Found: C, 75.95; H, 4.55, N, 11.05.

2.5.7. 3,3-dimethyl-12-phenyl-3,4,5,12-tetrahydrobenzo[4,5] imidazo-[2,1-b]quinazolin-1(2H)-one (6a)

m.p.: 234–236 °C; FT-IR (KBr) (ν_{max}/cm^{-1}): 3412 (N-H stretching), 3065 (aromatic C-H stretching), 2986 (aliphatic C-H stretching), 1739 (C=O stretching), 1609 (aromatic C=C stretching), 1571, 1456 (aromatic C=C stretching), 1346 (C-N stretching) cm^{-1}; ^{1}H NMR (DMSO-d_6, 300 MHz): δ_H (ppm) 0.97 (s, 3H, CH_3), 1.15 (s, 3H, CH_3), 2.21 (s, 2H, CH_2), 2.49 (s, 2H, CH_2), 4.65 (s, 1H, C-H), 7.21–7.34 (m, 2H), 7.45 (d, J = 8.2 Hz, 2H), 7.56–7.71 (m, 3H), 7.78 (t, J = 8.1 Hz, 2H), 11.31 (brs, N-H, 1H) ppm. ^{13}C NMR (DMSO-d_6, 75 MHz): δ_H (ppm) 15.45, 27.12, 29.21, 33.31, 51.43, 113.82, 114.23, 116.18, 121.69, 123.06, 124.75, 127.18, 128.42, 132.76, 136.54, 146.14, 146.87, 150.32, 196.38 (C=O) ppm. Anal Calc. for $C_{22}H_{21}N_3O$: C, 76.94; H, 6.16; N, 12.24. Found: C, 76.94; H, 6.16, N, 12.24.

2.5.8. 3,3-dimethyl-12-(4-nitrophenyl)-3,4,5,12-tetrahydrobenzo [4,5]imidazo-[2,1-b]quinazolin-1(2H)-one (6b)

m.p.: 257–259 °C; FT-IR (KBr) (ν_{max}/cm^{-1}): 3403 (N-H stretching), 3041 (aromatic C-H stretching), 2958 (aliphatic C-H stretching), 1743 (C=O stretching), 1616 (aromatic C=C stretching), 1571 (NO_2 stretching), 1463 (aromatic C=C stretching), 1363 (NO_2 stretching), 1344 (C-N stretching) cm^{-1}; ^{1}H NMR (DMSO-d_6, 300 MHz): δ_H (ppm) 0.91 (s, 3H, CH_3), 1.05 (s, 3H, CH_3), 2.12 (s, 2H, CH_2), 2.57 (s, 2H, CH_2), 4.64 (s, 1H, C-H), 7.47 (dd, J = 4.8 Hz, J = 6.9 Hz, 2H), 7.64 (d, J = 8.7 Hz, 3H), 8.11–8.16 (m, 3H), 11.31 (brs, N-H, 1H) ppm. ^{13}CNMR (DMSO-d_6, 75 MHz): δ_C (ppm) 15.45, 27.02, 29.03, 32.35, 50.35, 113.82, 123.60 (two peaks), 124.09 (two peaks), 128.86, 129.97 (two peaks), 146.42 (two peaks), 146.42, 152.26, 163.91, 196.50 (C=O) ppm. Anal Calc. for $C_{22}H_{20}N_3O_2$: C, 68.03; H, 5.19; N, 14.42. Found: C, 68.05; H, 5.11, N, 14.44.

2.5.9. 12-(1H-indol-3-yl-1H)-3,3-dimethyl-3,4,5,12-tetrahydrobenzo[4,5]imidazo-[2,1-b]quinazolin-1(2H)-one (6c)

m.p.: 221–223 °C; FT-IR (KBr) (ν_{max}/cm^{-1}): 3560, 3440 (N-H stretching), 2945 (aliphatic C-H stretching), 1685 (C=O stretching), 1616, 1460 (aromatic C=C stretching), 1379 (C-N stretching), 1107 cm^{-1}; ^{1}H NMR (DMSO-d_6, 300 MHz): δ_H (ppm) 0.99 (s, 6H), 2.11 (brs, 2H), 2.27 (brs, 2H), 4.75 (s, 1H, C-H), 7.00 (dd, J = 3.0 Hz, J = 5.7 Hz, 4H), 7.19–7.63 (m, 5H) ppm. ^{13}C NMR (DMSO-d_6, 75 MHz): δ_C (ppm) 14.44, 28.18, 31.16, 32.55, 50.74, 64.53, 101.40, 109.27, 110.14, 111.89, (two peaks), 116.14, 118.19, 121.12 (two peaks), 123.14 (two peaks), 123.14, 133.13, 133.94, 135.30, (two peaks), 153.79, 176.05 ppm. Anal Calc. for $C_{24}H_{22}N_4O$: C, 75.37; H, 5.58; N, 14.65. Found: C, 75.39; H, 5.59, N, 14.68.

2.5.10. 3,3-dimethyl-12-(4-chlorophenyl)-3,4,5,12-tetrahydrobenzo [4,5]imidazo-[2,1-b]quinazolin-1(2H)-one (6d)

m.p.: 199–201 °C; FT-IR (KBr) (ν_{max}/cm^{-1}): 3413 (N-H stretching), 3065 (aromatic C-H stretching), 2965 (aliphatic C-H stretching), 1767 (C=O stretching), 1606 (aromatic C=C stretching), 1571, 1478 (aromatic C=C stretching), 1344 (C-N stretching), 1021 (C-Cl stretch) cm^{-1}.^{1}H NMR (DMSO-d_6, 300 MHz): δ_H (ppm) 0.96 (s, 3H, CH_3), 1.15 (s, 3H, CH_3), 2.24 (s, 2H, CH_2), 2.67 (s, 2H, CH_2), 4.84 (s, 1H, C-H), 7.19–7.54 (m, 2H), 7.68 (d, J = 8.4 Hz, 3H), 8.01–8.26 (m, 3H) 11.31 (brs, N-H, 1H) ppm. ^{13}C NMR (DMSO-d_6, 75 MHz): δ_C (ppm) 18.76, 27.12, 28.13, 34.65, 51.55, 115.82, 120.60, 122.98, 125.01, 127.09, 129.87, 133.65, 145.12 (two peaks), 146.42, 147.56, 152.26, 167.01, 196.50 (C=O) ppm. Anal Calc. for $C_{22}H_{20}$ ClN_3O: C, 69.93; H, 5.33; N, 11.12. Found: C, 69.95H, 5.35, N, 11.11.

2.5.11. 3,3-dimethyl-12-(4-methoxyphenyl)-3,4,5,12-tetrahydrobenzo [4,5]imidazo-[2,1-b]quinazolin-1(2H)-one (6e)

m.p.: 234–235 °C; FT-IR (KBr) (ν_{max}/cm^{-1}): 3427 (N-H stretching), 3056 (aromatic C-H stretching), 2978 (aliphatic C-H stretching), 1746 (C=O stretching), 1610 (aromatic C=C stretching), 1485 (aromatic C=C stretching), 1344 (C-N stretching), 1211 (C-O stretch) cm^{-1}.^{1}H NMR (DMSO-d_6, 300 MHz): δ_H (ppm) 0.94 (s, 3H, CH_3), 1.15 (s, 3H, CH_3), 2.32 (s, 2H, CH_2), 2.76 (s, 2H, CH_2), 3.54 (s, 3H, OCH_3), 4.98 (s, 1H, C-H), 7.34 (d, J = 7.9 Hz, 2H), 7.54 (d, J = 8.2 Hz, 3H), 8.14–8.45 (m, 3H), 11.31 (brs, N-H, 1H) ppm. ^{13}CNMR (DMSO-d_6, 75 MHz): δ_C (ppm) 16.63, 27.12, 31.07, 35.35, 54.35, 58.12, 111.02, 123.60, 124.01, 124.09, 127.76, 128.86, 129.97, 132.78, 135.83, 148.42 (two peaks), 154.16, 165.98, 196.59 (C=O) ppm. Anal Calc. for $C_{23}H_{23}N_3O_2$: C, 73.97; H, 6.21; N, 11.25. Found: C, 73.96; H, 6.24, N, 11.29.

2.5.12. 3,3-dimethyl-12-(2-furyl)-3,4,5,12-tetrahydrobenzo [4,5] imidazo-[2,1-b]quinazolin-1(2H)-one (6f)

m.p.: 214–216 °C; FT-IR (KBr) (ν_{max}/cm^{-1}): 3409 (N-H stretching), 3068 (aromatic C-H stretching), 2978 (aliphatic C-H stretching), 1753 (C=O stretching), 1604 (aromatic C=C stretching), 1485 (aromatic C=C stretching), 1324 (C-N stretching), 1234 (C-O stretch) cm^{-1}.^{1}H NMR (DMSO-d_6, 300 MHz): δ_H (ppm) 0.96 (s, 3H, CH_3), 1.43 (s, 3H, CH_3), 2.32 (s, 2H, CH_2), 2.65 (s, 2H, CH_2), 4.96 (s, 1H, C-H), 7.26–7.64 (m, 3H), 7.74–7.91 (m, 2H), 8.11–8.25 (m, 2H), 11.33 (brs, N-H, 1H) ppm. ^{13}CNMR (DMSO-d_6, 75 MHz): δ_C (ppm) 15.82, 27.12, 31.07, 35.35, 54.35, 112.12, 121.40, 123.05, 125.00, 126.65, 127.06, 128.07, 130.08, 138.02, 141.09, 142.11, 154.16, 165.98, 196.59 (C=O) ppm. Anal Calc. for $C_{20}H_{19}N_3O_2$: C, 72.05; H, 5.74; N, 12.60. Found: C, 72.06; H, 5.74, N, 11.59.

2.5.13. 12-(1,3-diphenyl-1H-pyrazol-4-yl)-5H-benzo[4,5]imidazo [1,2-a]indeno[1,2-d]pyrimidin-13(12H)-one (5g)

m.p.: 221–223 °C; FT-IR (KBr) (ν_{max}/cm^{-1}): 3416 (N-H stretching), 3098 (aromatic C-H stretching), 2978 (aliphatic C-H stretching), 1747 (C=O stretching), 1611 (aromatic C=C stretching), 1563, 1476 (aromatic C=C stretching), 1356 (C-N stretching) cm^{-1}; ^{1}H NMR (DMSO-d_6, 300 MHz): δ_H (ppm) 5.35 (s, 1H), 6.86–6.96 (m, 3H), 7.15 (d, J = 8.3 Hz, 2H), 7.32–7.47 (m, 4H), 7.54 (d, J = 8.7 Hz, 3H), 7.61–7.68 (m, 3H), 7.78 (t, J = 8.2 Hz, 2H), 7.93 (s, 2H) ppm. ^{13}

CNMR (DMSO-d_6, 75 MHz): δ_C (ppm) 62.81, 107.12, 109.42, 111.09, 113.42, 115.65, 117.42 (two peaks), 118.13, 119.95, 120.09 (two peaks), 121.43, 123.34, 125.98, 130.02 (two peaks), 131.45, 133.19, 134.95 (two peaks), 135.11, 136.09, 138.90, 139.17, 141.17, 145.87, 195.73 ppm. Anal Calc. for $C_{32}H_{21}N_5O$: C, 78.19; H, 4.31; N, 14.25. Found: C, 78.16; H, 4.32, N, 14.26.

2.5.14. 12-(1-phenyl-3-(p-tolyl)-1H-pyrazol-4-yl)-5H-benzo[4,5] imidazo[1,2-a]indeno[1,2-d]pyrimidin-13(12H)-one (5 h)

m.p.: 254–256 °C; FT-IR (KBr) (v_{max}/cm^{-1}): 3445 (N-H stretching), 3087 (aromatic C-H stretching), 2989 (aliphatic C-H stretching), 1783 (C=O stretching), 1604 (aromatic C=C stretching), 1587, 1487 (aromatic C=C stretching), 1343 (C-N stretching) cm^{-1}; ^{1}H NMR (DMSO-d_6, 300 MHz): δ_H (ppm) 2.54 (s, 3H), 5.41 (s, 1H), 7.07–7.25 (m, 5H), 7.43 (d, J = 8.2 Hz, 2H), 7.54 (t, J = 8.1 Hz, 3H), 7.62–7.76 (m, 4H), 7.83 (brs, 3H), 7.89–7.96 (m, 1H) ppm. ^{13}C NMR (DMSO-d_6, 75 MHz): δ_C (ppm) 43.17, 62.98, 108.43, 110.02, 111.45, 113.58, 114.73, 117.42, 118.09, 119.16, 119.45, 120.54, 121.87, 122.45, 127.18, 130.12, 131.98, 132.87, 132.99, 133.55, 134.21, 135.09, 137.91, 138.46, 139.18, 145.17, 145.76, 195.73 ppm. Anal Calc. for $C_{33}H_{23}N_5O$: C, 78.40; H, 4.59; N, 13.85. Found: C, 78.43; H, 4.56, N, 13.86.

2.5.15. 12-(1,3-diphenyl-1H-pyrazol-4-yl)-3,3-dimethyl-3,4,5,12-tetrahydro benzo [4,5] imidazo [2,1-b]quinazolin-1(2H)-one(6g)

m.p.: 211–212 °C; FT-IR (KBr) (v_{max}/cm^{-1}): 3427 (N-H stretching), 3076 (aromatic C-H stretching), 2987 (aliphatic C-H stretching), 1747 (C=O stretching), 1609 (aromatic C=C stretching), 1555, 1487 (aromatic C=C stretching), 1348 (C-N stretching) cm^{-1}; ^{1}HNMR (DMSO-d_6, 300 MHz): δ_H (ppm) 0.97 (s, 3H, CH_3), 1.15 (s, 3H, CH_3), 2.54 (s, 2H, CH_2), 2.59 (s, 2H, CH_2), 4.76 (s, 1H, C-H), 7.09–7.23 (m, 2H), 7.34 (t, J = 8.2 Hz, 3H), 7.42–7.49 (m, 3H), 7.56-7.68 (m, 4H), 7.83 (brs, 3H), 11.31 (brs, N-H, 1H) ppm. ^{13}C NMR (DMSO-d_6, 75 MHz): δ_C (ppm) 20.12, 22.32, 28.53, 31.43, 52.12, 111.28, 114.89, 119.21, 121.09, 123.45, 124.09 (two peaks), 125.34, 127.81, 128.66, 128.99, 131.22, 135.62, 138.43, 139.11, 143.22 (two peaks), 146.42, 163.91, 196.50 (C=O) ppm. Anal Calc. for $C_{31}H_{27}N_5O$: C, 76.68; H, 5.60; N, 14.42. Found: C, 76.67; H, 5.63, N, 14.41.

2.5.16. 3,3-dimethyl-12-(1-phenyl-3-(p-tolyl)-1H-pyrazol-4-yl)-3,4,5,12-tetrahydrobenzo[4,5]imidazo[2,1-b]quinazolin-1(2H)-one (6 h)

m.p.: 287–288 °C; FT-IR (KBr) (v_{max}/cm^{-1}): 3432 (N-H stretching), 3065 (aromatic C-H stretching), 2987 (aliphatic C-H stretching), 1753 (C=O stretching), 1602 (aromatic C=C stretching), 1548, 1464 (aromatic C=C stretching), 1346 (C-N stretching) cm^{-1}; ^{1}H NMR (DMSO-d_6, 300 MHz): δ_H (ppm) 0.99 (s, 3H, CH_3), 1.11 (s, 3H, CH_3), 2.25–2.43 (m, 4H), 2.49 (s, 3H, CH_3), 4.79 (s, 1H, C-H), 7.19–7.29 (m, 4H), 7.54 (s, 2H), 7.62–7.69 (m, 3H), 7.87 (d, J = 8.4 Hz, 3H), 8.01–8.21 (m, 2H) ppm. ^{13}C NMR (DMSO-d_6, 75 MHz): δ_C (ppm) 19.32, 27.16, 29.41, 32.63, 45.66, 51.14, 111.98, 112.21, 114.65, 117.75, 119.11, 120.11, 123.15, 123.87, 124.36, 126.11, 127.69, 131.43, 13.72, 136.69, 137.42, 139.12, 143.22, 145.75, 146.42, 163.91, 196.50 (C=O) ppm. Anal Calc. for $C_{32}H_{29}N_5O$: C, 76.93; H, 5.85; N, 14.02. Found: C, 76.97; H, 5.83, N, 14.03.

3. Results and discussion

3.1. Synthesis and structural characterization of L-proline functionalized-propyl mediated nano magnetic (Fe_3O_4@SiO_2@L-proline)

In continuation of our research for the green synthesis of organic compounds [23–31], herein, we wish to report the synthesis of Fe_3O_4@SiO_2@L-proline nano particles and their characterization and application for the synthesis benzimidazo[1,2-*a*] pyrimidinone and tetrahydrobenzo[4,5]imidazo-[1,2-*d*]quinazolin-1(2*H*)-one and their derivatives bearing different functional groups with significant convenience.

As shown in Scheme 1, the Fe_3O_4@SiO_2@L-proline magnetic nanoparticles were synthesized in three steps from commercially available materials. Fe_3O_4 NPs were coated by silica using a sol–gel process. The Fe_3O_4@SiO_2 core-shell structures were then sequentially treated with 3-chloropropyltrimethoxysilane. Next, it was treated with L-proline to obtain the L-proline coated on the propyl mediated nano magnetic.

The morphology and nanoparticle size of the synthesized

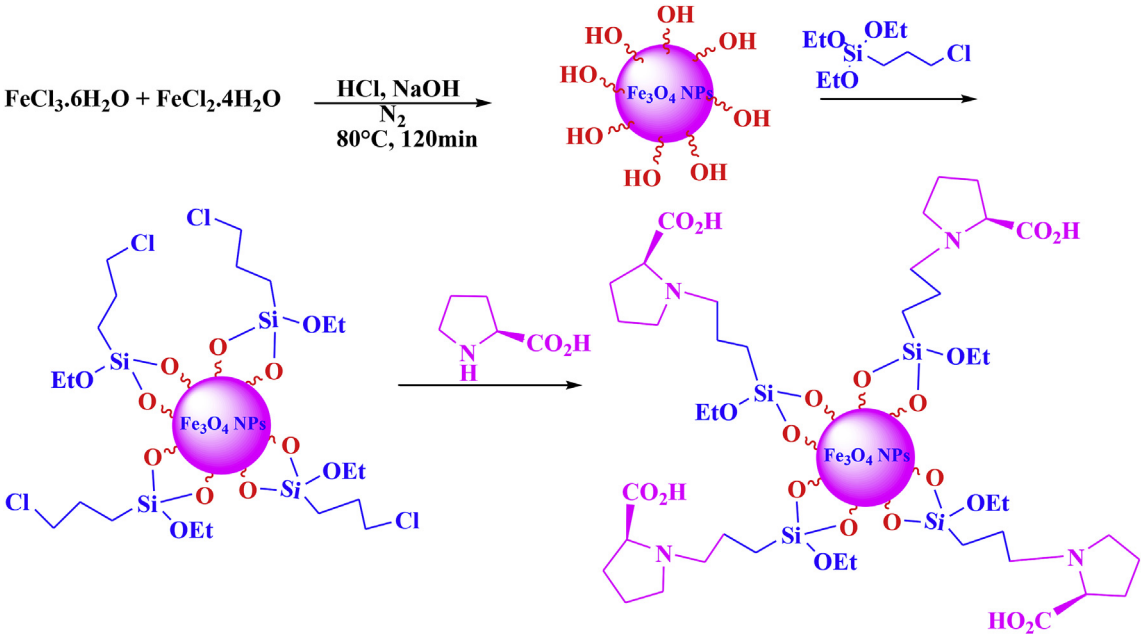

Scheme 1. Stepwise synthesis pathway of Fe_3O_4@SiO_2@L-proline

magnetic catalyst were characterized by transmission electron microscope (TEM) and Field Emission Scanning Electron Microscope (Fe-SEM) (Fig. 1). As shown in Fig. 1, TEM and Fe-SEM images of the Fe_3O_4@SiO_2@L-proline catalyst reveal that Fe_3O_4@SiO_2@L-proline nanoparticles are formed with nearly spherical morphology having a particle size of 8–13 nm. Furthermore, TEM images show some aggregation, which was illustrated the successful grafting of the polymer on magnetic nanoparticles.

XRD analysis of the Fe_3O_4@SiO_2@L-proline catalyst in contract to pure Fe_3O_4 [31] (powder form) confirms the formation of Fe_3O_4-NPs. This pattern shows characteristic peaks at 20, 30, 35.2, 43.1, 56.9, 59.8, 62.7 and 74.3. These peaks are indicative of the pure face-centred cubic structure of Fe_3O_4 (Fig. 2a). The characteristic peak of SiO_2 and L-proline in the core shell structure is hidden under a weak peak of Fe_3O_4 at $2\theta = 30$ and 62.7, respectively.

The results of energy dispersive X-ray spectroscopy (EDX) analysis of the synthesized Fe_3O_4@SiO_2@L-proline MNPs proved existence of Fe (32.08 w/w %), O (47.35 w/w %), Si (6.31 w/w %), N (1.29 w/w %) and C (12.66 w/w %) atoms in the structure that confirms the presence of Fe_3O_4 core in the structure of MNP. The results are summarized in Fig. 2b.

FT-IR measurement of Fe_3O_4@SiO_2@L-proline (Fig. 2c) was conducted to identify the functional groups of the synthesized nanoparticles. The strong intense band at 1729 cm^{-1} corresponds to the C=O stretching mode of carboxylic acid, which indicates the presence of L-proline. The broad band at 3100-3600 cm^{-1} are

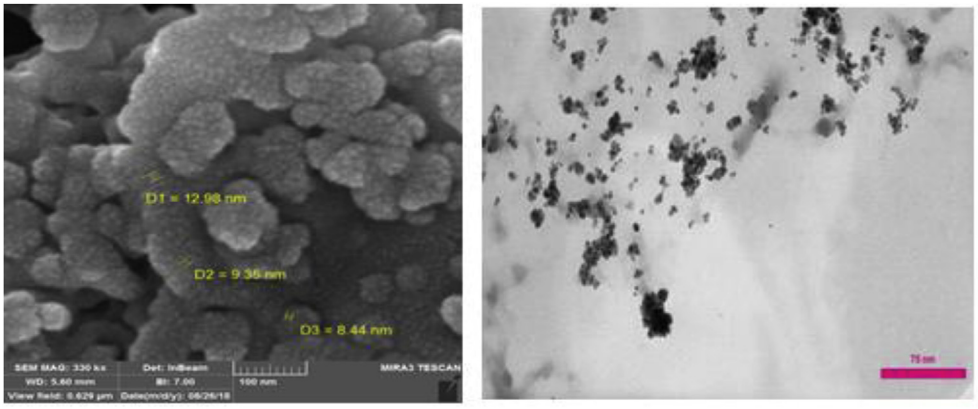

Fig. 1. a) Left: Fe-SEM and b) right: TEM image of synthesized Fe_3O_4@SiO_2@L-proline

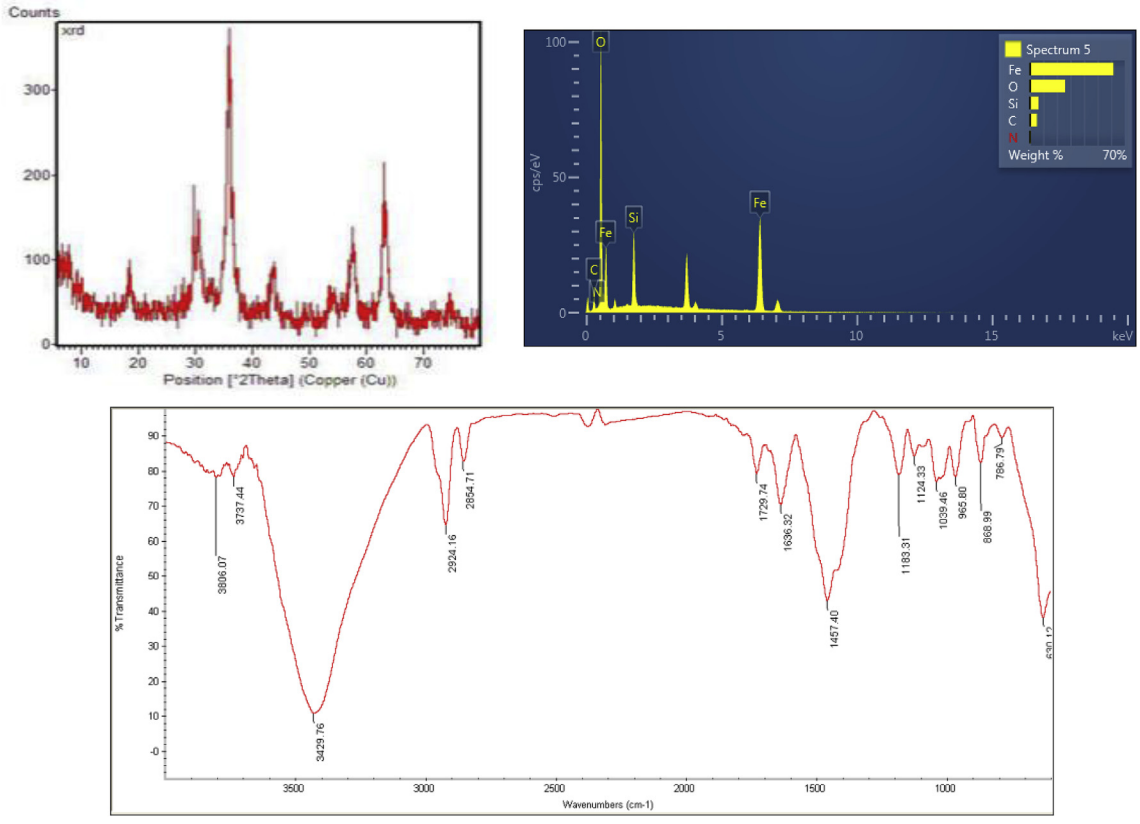

Fig. 2. a) left: XRD analysis of the Fe_3O_4@SiO_2@L-proline, b) right: EDX analysis, c) down: FT-IR spectrum.

assigned to OH stretching vibrations of carboxylic acid moiety. The band centred at 1039 and 786 cm^{-1} are associated with Si-O-Si vibrations in SiO_2 shell.

VSM measurements (Fig. 3a) were carried out at room temperature by taking the solid sample on the tips of the vibrating rod and analyzing in an applied magnetic field sweeping from −10 to 10 kOe. The curve confirms the magnetic property of the synthesized nanoparticle is in agreement with the other studies [32].

In order to investigate the thermal stability of the synthesized nano catalyst, thermal gravimetric and derivative thermal gravimetric analysis (TGA and DTG) of the Fe_3O_4@SiO_2@L-proline MNPs were carried out from 50 to 700 °C at a heating rate of 10 °C min^{-1} under air atmosphere (Fig. 3b). TGA plot for NPs can prove the thermal stability of the synthesized nanoparticles. The thermal stability is due to the presence of Fe_3O_4 and SiO_2 in the core−shell system. TGA curve of Fe_3O_4@SiO_2@L-proline MNPs showed a 12.5 % weight loss from 25 to 700 °C. In DTG curve, with increasing the temperature up to 200 °C, a little weight loss (7 wt%) was observed with a maximum in 123 °C (from DTG) that could be due to the removal of physically adsorbed water and unreacted organic molecules which were adsorbed during the synthesis of nanoparticles. Further increase in temperature from 250 to 450 °C, showed a second weight loss (2.5 wt %) due to the decomposition of L-proline from the surface of silanol group (with the highest rate at 386 °C). After increasing the temperature up to 700 °C, a further decrease in weight (2.5 wt %) was observed between 450 and 700 °C that can be related to the decomposition of propyl moiety from the surface of MNPs.

To investigation the surface charge of MNPs and their stability in solution, zeta potential values were measured using the Zeta sizer instrument. This value can be explain tendency to aggregate in solution. In the present study, the zeta potential and mobility were measured as −45.3 mv and −2.50 μmcm/Vs, respectively at 298 K with count rate of 94.4 kcps (Fig. 4). The large zeta potential obtained in this study predicts a more stable dispersion of synthesized MNPs.

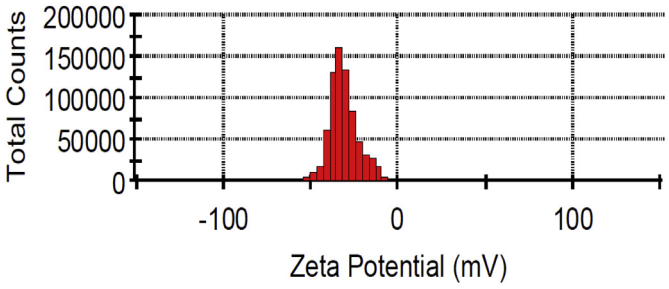

Fig. 4. Zeta potential of synthesized Fe_3O_4@SiO_2@L-proline

3.2. Catalytic studies

The activity of the catalyst was then investigated by employing it in the multicomponent synthesis of benzimidazo [1,2-*a*]pyrimidinone and tetrahydrobenzo[4,5]imidazo-[1,2-*d*]quinazolin-1(2*H*)-one using multicomponent reaction of various benzaldehyde, dimedone or indandione and 2-aminobenzimidazole in aqeous media at room temperature (Scheme 2).

To find the best conditions, the reaction between 4-nitrobenzaldehyde, indanedione and 2-aminobenzimidazole was chosen as a model reaction, for which the influences of various parameters as reaction temperature, solvent, amount of catalyst were examined to obtain the best possible combination (Table 1). Initially, a series of solvents, including H_2O, DMF, EtOH, CH_3CN, H_2O−EtOH (1:1), toluene and in the absence of solvent (solvent-free condition) were studied in the presence of 0.05 g of prepared catalyst. The best result was obtained in aqueous media (Table 1, entry 7). Next, the effects of catalyst loading under the aqueous condition and the effect of temperature on the model reaction were examined. The results were summarized in Table 1. The best results were gained with 0.05 g catalyst in aqueous media at room temperature. The rising of temperature and the addition of more catalyst amount didn't lead to better results (reaction time and yield).

The scope of the reaction was then expanded to various benzaldehydes including a range of eletron-releasing or electron-withdrawing elements (Table 2). As shown in Table 2 both electron-donating and electron withdrawing groups lead to the corresponding products in excellent yields.

A plausible mechanism was proposed in Fig. 5. Initially, Fe_3O_4@SiO_2@L-proline activates benzaldehydes, then the condensation reaction of indanedione **3** with activated aldehydes and dehydration produced chalcone **9**. Then, the Michael reaction of chalcone with 2-aminobenzimidazole and dehydration lead to product **5**.

The reusability of the catalyst is another important factor from economic and environmental points of view. After completion of reaction, the nano catalysts were isolated from the mixture of the reaction by simple filtration in the presence of an enormous magnetic bar and reused ten times after washing with ethanol and drying. The results of recycling of the catalyst for 5a were

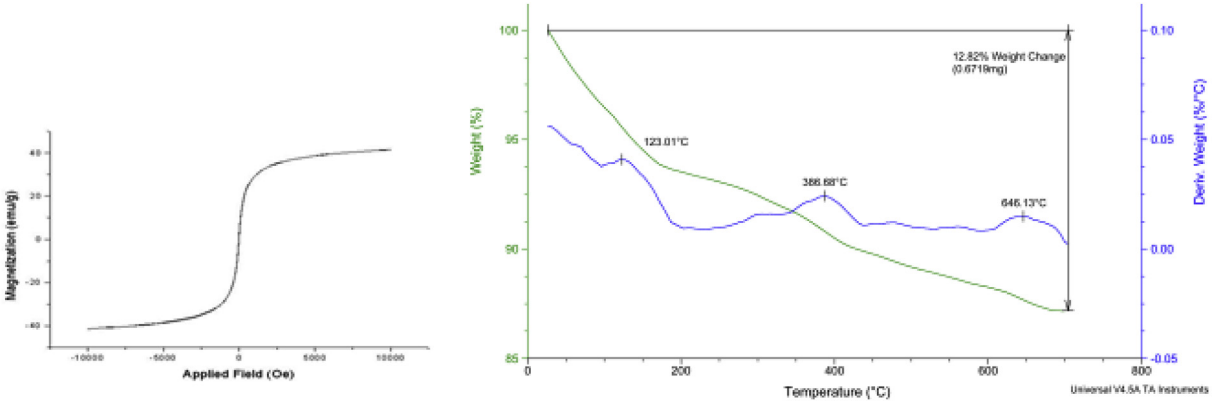

Fig. 3. a) Left: VSM measurements of Fe_3O_4@SiO_2@L-proline MNPs, b) right: Thermogram of TGA (green colour) and DTG (blue colour). (For interpretation of the references to colour in this figure legend, the reader is referred to the Web version of this article.)

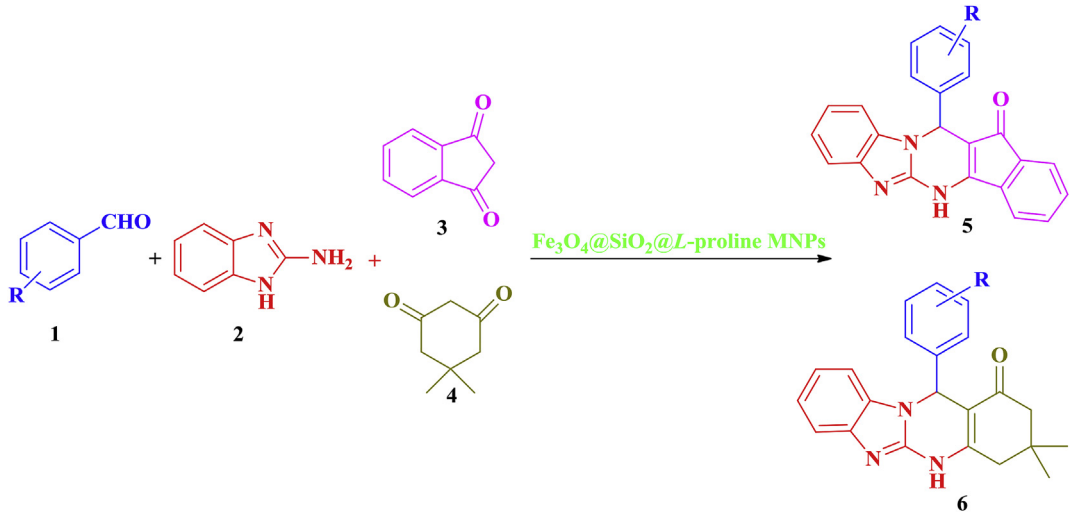

Scheme 2. Multicomponent synthesis of benzimidazo [1,2-a] pyrimidinone and tetrahydrobenzo[4,5]imidazo-[1,2-d]quinazolin-1(2H)-one using Fe_3O_4@SiO_2@*L*-proline MNPs.

summarized in chart. The TEM image and XRD analysis of recycled nano catalyst was shown in Fig. 6.

In continuation of our effort to synthesize pyrazolyl moiety of these compounds, we concentrated for the synthesis of **5g**, **5h**, **6g** and **6h** as shown in Fig. 7.

In order to demonstrate the potential application of this route, the reaction was carried out on a gram scale. As shown in Scheme 3, when 1.51 g of 4-nitrobenzaldehyde was used under the standard conditions, the product 5a was obtained in 97% yield with the reaction time prolonged to 13min, indicating that this route could be scaled up to a preparing scale.

4. Conclusion

This paper introduces a novel nano magnetically Brønsted acid catalyst Fe_3O_4@SiO_2@*L*-proline and evaluates its efficiency for the multicomponent synthesis of benzoimidazo[1,2-*a*]pyrimidine and tetrahydrobenzo [4,5]imidazo[2,1-*b*]quinazolin-1(2*H*)-one using aldehyde, dimedone or indanedione and 2-aminobenzimidazole in simple condition. It has also been demonstrated that Fe_3O_4@-SiO_2@*L*-proline can be employed as a green, reusable and efficient heterogeneous nano catalyst in these transformations. This protocol has several advantages including simple reaction conditions,

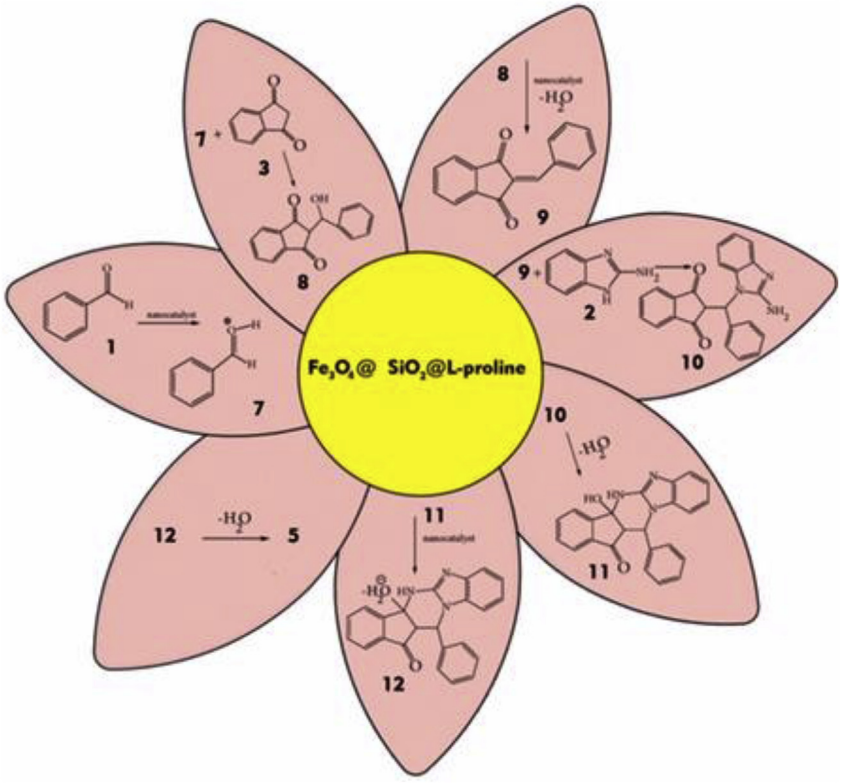

Fig. 5. Proposed mechanistic pathway for the synthesis of benzimidazo [1,2-a]pyrimidinone using Fe_3O_4@SiO_2@L-proline MNPs.

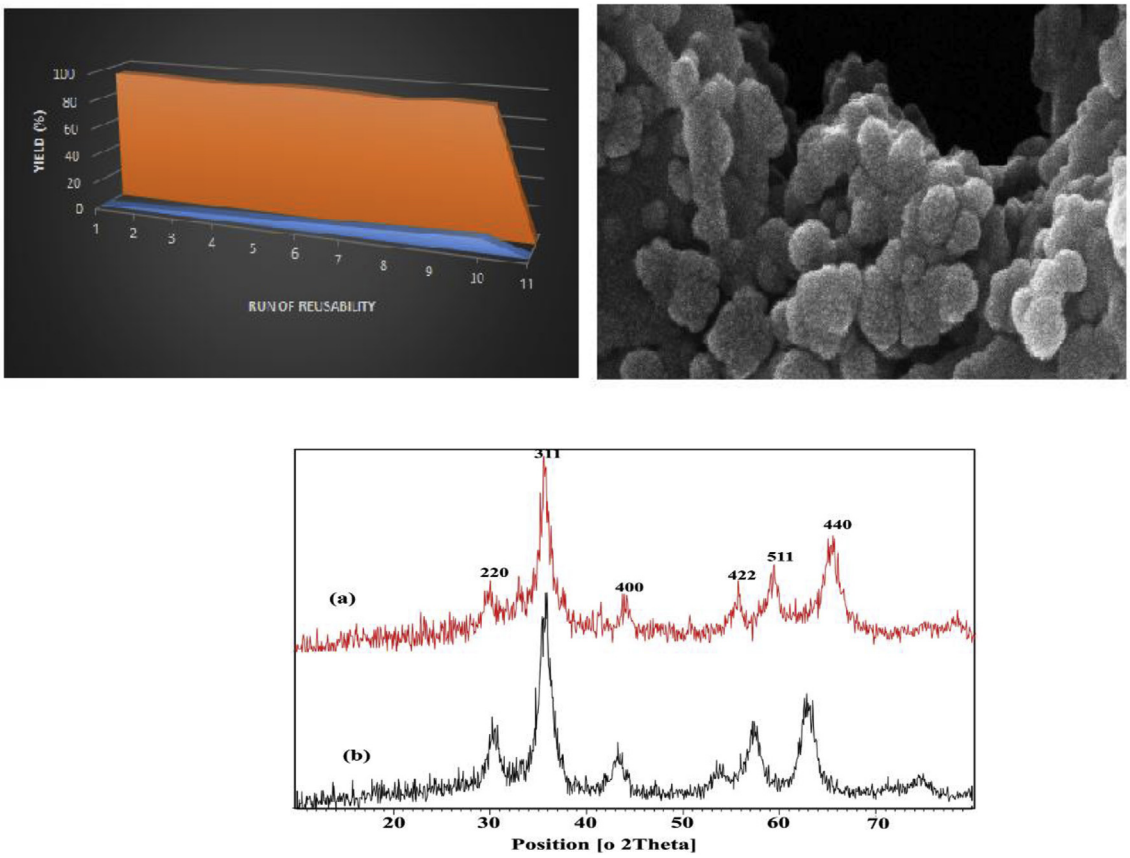

Fig. 6. up) left: The reusability of synthesized catalyst, right: Fe-SEM image of recycled nanocatalyst, down) XRD analysis of recycled nanocatalyst after ten cycles.

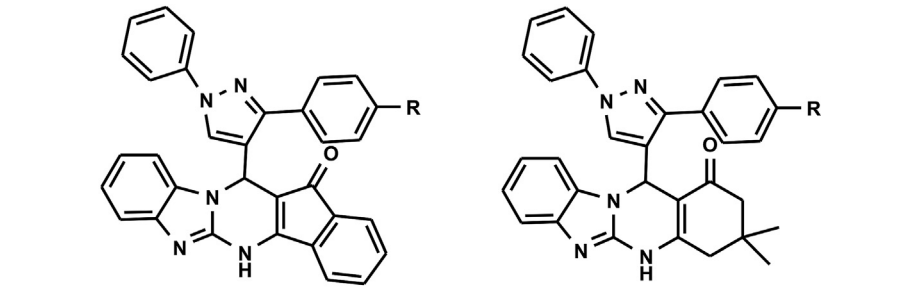

5g, R = H, 10min, 96%, mp = 221-223 °C
5h, R = CH_3, 15min, 92%, mp = 254-256°C

6f, R = H, 15min, 98%, mp = 211-212°C
6g, R = CH_3, 20min, 96%, mp = 287-88°C

Fig. 7. Synthesis of new category of synthesized pyrazolyl moiety compounds.

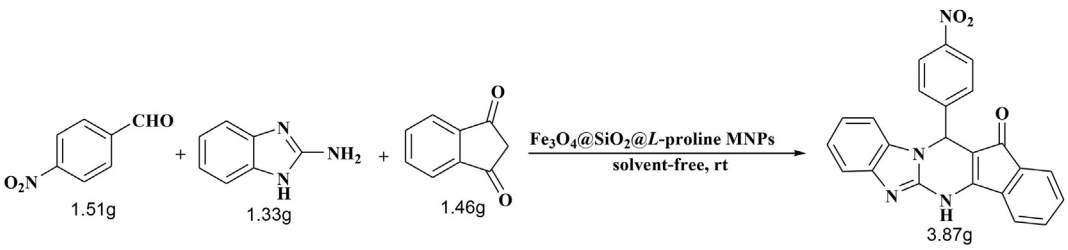

Scheme 3. The gram scale estimation of this avenue for 5a.

simplicity of operation, short reaction times, practicability, good to high yields and using an eco-friendly, commercially available, cheap and chemically stable catalyst. Recyclability through applying an external magnetic field and excellent chemoselectivity are the other advantages of this avenue.

Acknowledgements

Financial support by Payame Noor and Ghadr University, Islamic Azad university of Rasht branch especially Dr Shahab Shariati is gratefully acknowledged.

References

[1] A.A.M. Abdel-Hafez, Arch Pharm. Res. (Seoul) 30 (2007) 678–684.
[2] (a) B. Cosimelli, S. Laneri, C. Ostacolo, A. Sacchi, E. Severi, E. Porcu, E. Rampazzo, E. Moro, G. Basso, G. Viola, Eur. J. Med. Chem. 83 (2014) 45–56; (b) A. Linton, P. Kang, M. Ornelas, S. Kephart, Q. Hu, M. Pairish, Y. Jiang, C. Guo, J. Med. Chem. 54 (2011) 7705–7712.
[3] Y. Rival, G. Grassy, A. Taudou, R. Ecalle, Eur. J. Med. Chem. 26 (1991) 13–18.
[4] A. Vidal, M.L. Ferrándiz, A. Ubeda, A. Acero-Alarcón, J. Sepulveda-Arques, M.J. Alcaraz, Inflamm. Res. 50 (2001) 317–320.
[5] A. Gueiffier, M. Lhassani, A. Elhakmaoui, R. Snoeck, G. Andrei, O. Chavignon, J.C. Teulade, A. Kerbal, E.M. Essassi, J.C. Debouzy, M. Witvrouw, Y. Blache, J. Balzarini, E.D. Clercq, J.P. Chapat, J. Med. Chem. 39 (1996) 2856–2859.
[6] Y. Rival, G. Grassy, G. Michel, Chem. Pharm. Bull. 40 (1992) 1170–1176.
[7] N. Margiotta, R. Ostuni, R. Ranaldo, N. Denora, V. Laquintana, G. Trapani, G. Liso, G. Natile, J. Med. Chem. 50 (2007) 1019–1027.
[8] P.J. Sanfilippo, M. Urbanski, J.B. Press, B. Dubinsky, J.B. Moore, J. Med. Chem. 31 (1998) 2221–2227.
[9] J. Jiricek, F. Liang, C.J.N. Mathison, P.K. Mishra, V. Molteni, A.S. Nagle, F. Supek, L.J. Tan, A. Vidal, V. Yeh, PCT Int. Appl. (2014). WO2014151784 A1.
[10] W.R. Tully, C.R. Gardner, R.J. Gillespie, R. Westwood, J. Med. Chem. 34 (1991) 2060–2067.
[11] (a) K. Nacro, A.J. Duraiswamy, L.R. Chennamaneni, PCT Int. Appl. (2013). WO2013147711 A1; (b) K.C. Rupert, J.H. Henry, J.H. Dodd, S.A. Wadsworth, D.E. Cavender, G.C. Olini, B. Fahmy, J.J. Siekierka, Bioorg. Med. Chem. Lett 13 (2003) 347–350.
[12] J. J. Nunes, X.T. Zhu, M. Ermann, C. Ghiron, D. N. Johnston, C. G. P. Saluste, W.O. Patent 2005021551, 2005.
[13] M. Cheung, P. A. Harris, M. Hasegawa, S. Ida, K. Kano, N. Nishigaki, H. Sato, J. M. Veal, Y. Washio, R. I. West, W.O. Patent 2002044156, 2002.
[14] J. J. Nunes, X. T. Zhu, P. Amouzegh, C. Ghiron, D. N. Johnston, E. C. Power, W.O. Patent 2005009443, 2005.
[15] (a) D. Descours, D. Festal, Synthesis (1983) 1033–1036; (b) J.L. LaMattina, C.J. Mularski, D.E. Muse, Tetrahedron 44 (1988) 3073–3078.
[16] (a) W. Nawrocka, Pol. J. Chem. 69 (1995) 1158–1169; (b) N. Zanatta, S.S. Amaral, A. Esteves-Souza, A. Echevarria, P.B. Brondani, D.C. Flores, H.G. Bonacorso, A.F.C. Flores, M.P. Martins, Synthesis (2006) 2305–2312.
[17] C.S. Yao, S. Lei, C.H. Wang, C.X. Yu, Q.Q. Shao, S.J. Tu, Chin. J. Chem. 26 (2008) 2107–2111.
[18] A. Shaabani, A. Rahmati, S. Naderi, Bioorg. Med. Chem. Lett 15 (2005) 5553–5557.
[19] (a) P.F. Asobo, H. Wahe, J.T. Mbafor, A.E. Nkengfack, Z.T. Fomum, E.F. Sopbue, D. Dopp, J. Chem. Soc. Perkin Trans 1 (2001) 457–461; (b) A. Da Settimo, G. Primofiore, F. Da Settimo, A.M. Marini, S. Taliani, S. Salermo, L.D. Via, J. Heterocycl. Chem. 40 (2003) 1091–1096; (c) F. Karci, A. Demircali, I. Sener, T. Tilki, Dyes Pigments 71 (2006) 90–96; (d) F. Troxler, H.P. Weber, Helv. Chim. Acta 57 (1974) 2356–2361.
[20] (a) D. Basavaiah, K.V. Rao, R. Reddy, J. Chem. Soc. Rev. 36 (2007) 1581–1588; (b) V. Singh, S. Batra, Tetrahedron 64 (2008) 4511–4574; (c) K.Y. Lee, S. Gowrisankar, J.N. Kim, Bull. Korean Chem. Soc. 26 (2005) 1481–1490; (d) Y.L. Shi, M. Shi, Org. Biomol. Chem. 5 (2007) 1499–1504; (e) D. Basavaiah, A.J. Rao, T. Satyanarayana, Chem. Rev. 103 (2003) 811–892.
[21] A. Molnar, Chem. Rev. 111 (2011) 2251–2320.
[22] (a) A.P. Wight, M.E. Davis, Chem. Rev. 102 (2002) 3589–3614; (b) J. Mondal, T. Sen, A. Bhaumik, Dalton Trans. 41 (2012) 6173–6181; (c) P. Das, A. Dutta, A. Bhaumik, Ch Mukhupadhyay, Green Chem. 16 (2014) 1426–1435.
[23] M. Nikpassand, L.Z. Fekri, A. Pourahmad, J. CO_2. Utiliz. 27 (2018) 320–325.
[24] L.Z. Fekri, M. Nikpassand, S. Pourmirzajani, B. Aghazadeh, RSC Adv. 8 (2018) 22313–22320.
[25] L.Z. Fekri, M. Nikpassand, S. Shariati, B. Aghazadeh, R. Zarkeshvari, J. Org. Met. Chem. 871 (2018) 60–73.
[26] L.Z. Fekri, M. Nikpassand, R. Maleki, J. Mol. Liq. 222 (2016) 77–81.
[27] S. Farshbaf, L.Z. Fekri, M. Nikpassand, R. Mohammadi, E. Vessally, J. CO_2. Utiliz. 25 (2018) 194–204.
[28] L. Zare, N.O. Mahmoodi, A. Yahyazadeh, M. Mamaghani, K. Tabatabaeian, Chin. Chem. Lett. 21 (2010) 538–541.
[29] A. Hosseinian, S. Farshbaf, L.Z. Fekri, M. Nikpassand, E. Vessally, Top. Curr. Chem. 23 (2018) 376–383.
[30] M. Nikpassand, L.Z. Fekri, S. Sanagou, Dyes Pigments 136 (2017) 140–144.
[31] L. Zare, N. Mahmoodi, A. Yahyazadeh, M. Mamaghani, K. Tabatabaeian, J. Heterocycl. Chem. 48 (2011) 864–867.
[32] M.K. Ahmadi, M. Vossoughi, J. Nanotech 1 (2013) 7–13.